Self-induced fractional Fourier transform and revivable higher-order spatial solitons in strongly nonlocal nonlinear media

Daquan Lu, Wei Hu,* Yajian Zheng, Yanbin Liang, Longgui Cao, Sheng Lan, and Qi Guo
Laboratory of Photonic Information Technology, South China Normal University, Guangzhou 510631, China
(Received 14 June 2008; published 14 October 2008)

The fractional Fourier transform (FRFT) naturally exists in strongly nonlocal nonlinear (SNN) media and the propagation of optical beams in SNN media can be simply regarded as a self-induced FRFT. Through the FRFT technique the evolution of fields in SNN media can be conveniently dealt with, and an arbitrary square-integrable input field presents itself generally as a revivable higher-order spatial soliton which reconstructs its profile periodically after every four Fourier transforms. The self-induced FRFT illuminates the prospects for SNN media in new applications such as continuously tunable nonlinearity-induced FRFT devices.

DOI: 10.1103/PhysRevA.78.043815 PACS number(s): 42.65.Tg, 42.30.Kq, 42.65.Jx

Since Fourier suggested the usage of Fourier analysis to solve the heat conduction problem in 1807, the Fourier transform (FT) has been applied widely in many branches of science [1]. In the field of optics, the FT is one of the most important and basic tools in dealing with physical optics and optical information processing [1]. In fact, the term Fourier optics is often used synonymously with optical information process. The fractional Fourier transform (FRFT), which is an extension of the FT [2], was introduced to optics in 1993, when Mendlovic and Ozaktas found that this operation can be optically performed by quadratic graded-index (GRIN) media [3]. Because the FRFT can show the characteristics of the signal changing continuously from the spatial domain to the spectral domain, it interests optical scientists and engineers and plays an important role in many optics fields [4–12], such as diffraction [7], transmission [8,9], imaging [10], information processing [11,12], etc.

On the other hand, since the first observation of nonlinear optical phenomena by Franken *et al.* in 1961 [13], one year after the invention of the laser, nonlinear optics has been a rapidly expanding active field and has widely influenced other fields. A special branch of nonlinear optics, the field of optical solitons, has grown enormously in recent decades. In particular, the solitons in strongly nonlocal nonlinear (SNN) media, which support (2+1)-dimension solitons, have attracted extensive interest and been widely investigated in the past few years [15–27], since Snyder and Mitchell simplified the nonlocal nonlinear Schrödinger equation (NNLSE) to a linear model [called the Snyder-Mitchell mode (SMM) here] in the SNN case and found an exact Gaussian-shaped "accessible soliton"[14]. The accessible soliton is interesting for potential applications such as photonic switching and logic gating [27].

Fourier optics and nonlinear optics might seem to be independent of each other in that the FT and the FRFT are linear transforms and well known as techniques to solve problems in linear systems. But we note that SNN media, where the propagation equation can be mathematically simplified to the linear SMM [14], would provide an opportunity for them to intersect with each other.

In this paper, a FRFT induced by the input field itself through the SNN effect is introduced. It is shown that the FRFT naturally exists in SNN media. The order of the self-induced FRFT in SNN media can be steered using the input power in addition to the propagation distance z, quite unlike the traditional linear (intensity-independent) FRFT devices such as the lens series and the quadratic GRIN media. Due to the self-induced FRFT, propagation of an arbitrary square-integrable input field presents itself generally as a *revivable higher-order spatial soliton* (RHOSS) which is similar to the higher-order (1+1)-dimensional temporal soliton in a fiber. The building-block-like solitons, building-block-like breathers, and their interaction, can be regarded as special cases of the RHOSS and can be conveniently investigated with the FRFT technique.

The propagation of beams in nonlocal nonlinear media can be phenomenologically described by the NNLSE: $2ikn_0\partial_z\Phi+n_0\Delta_\perp\Phi+2k^2\Delta n\Phi=0$, where k represents the wave number in a medium with the linear part of the refractive index n_0 when the nonlinear perturbation of the refractive index, Δn, equals zero, $\Delta n=n_2\int R(\vec{r}-\vec{r}_a)|\Phi|^2d^2\vec{r}_a$ (n_2 is the nonlinear index coefficient and R is the normalized symmetric real spatial response function of the medium). In the case of SNN media we need only keep the first two terms of the expansion of Δn and the NNLSE is simplified to the SMM [14],

$$2ik\partial_z\Phi+\Delta_\perp\Phi-k^2\gamma^2P_0r^2\Phi=0, \tag{1}$$

where γ is a material constant and $P_0=\int|\Phi|^2d^2\vec{r}$ is the input power.

We assume $\Phi(\vec{r},z)=a(\vec{r})\exp(-i\beta z)$ to seek the stationary solutions of Eq. (1). Substituting this expression into Eq. (1) gives $2\beta ka=k^2\gamma^2P_0r^2a-\Delta_\perp a$, the eigensolutions of which are the Hermite Gaussian soliton family

$$a^{(p)}=\mathcal{H}_{m,n}^{(p)}=c^{(p)}H_m\left(\frac{x}{w_c}\right)H_n\left(\frac{y}{w_c}\right)e^{-r^2/2w_c^2}\quad(m+n=p) \tag{2}$$

in Cartesian coordinates [26], the Laguerre Gaussian soliton family

*huwei@scnu.edu.cn

 ©2008 The American Physical Society

$$a^{(p)} = \begin{cases} \mathcal{L}_{l,q}^{c(p)} = c^{(p)}\left(\frac{r}{w_c}\right)^l L_q^l\left(\frac{r}{w_c}\right)\cos(l\theta)e^{-r^2/2w_c^2}, \\ \mathcal{L}_{l,q}^{s(p)} = c^{(p)}\left(\frac{r}{w_c}\right)^l L_q^l\left(\frac{r}{w_c}\right)\sin(l\theta)e^{-r^2/2w_c^2} \quad (2q+l=p) \end{cases} \tag{3}$$

in circular cylindrical coordinates [26], or the Ince Gaussian soliton family in elliptical coordinates [23,24]. In Eqs. (2) and (3), $p=0,1,2,\ldots$ is the order of the solution with which the soliton eigenvalue can be straightforwardly obtained:

$$\beta^{(p)} = (p+1)\beta_0, \tag{4}$$

$c^{(p)}$ is the normalized coefficient ensuring that $\int|a^{(p)}|^2 d^2\vec{r} = P_0$, $w_c=(k^2\gamma^2 P_0)^{-1/4}$ is a generalized beamwidth, $H_m(x)$ and $L_q^l(r)$, respectively, represent the Hermite and Laguerre polynomials, and $\beta_0=\sqrt{P_0\gamma}=1/kw_c^2$.

Mathematically, the profile of the eigensoliton solution $a^{(p)}$ is simultaneously the eigenfunction of the FRFT [2–4],

$$\hat{F}_\alpha\{g(\vec{r}_1)\}(\vec{r}_2) = \frac{\exp[i(\alpha-\pi/2)]}{2\pi w_c^2 \sin\alpha} \times\exp\left(\frac{ir_2^2}{2w_c^2\tan\alpha}\right) \times\int\exp\left(\frac{ir_1^2}{2w_c^2\tan\alpha} - \frac{i\vec{r}_1\cdot\vec{r}_2}{w_c^2\sin\alpha}\right)g(\vec{r}_1)d^2\vec{r}_1,$$

i.e., $a^{(p)}$ is the eigensolution of the equation $\hat{F_\alpha}\{a^{(p)}(\vec{r}_1)\} = a^{(p)}(\vec{r}_2)e^{-ip\alpha}$ with the eigenvalue $e^{-ip\alpha}$, where the order of the FRFT is

$$\alpha = \beta_0 z = \sqrt{P_0}\gamma z. \tag{5}$$

Therefore the field of the eigensoliton at z is connected with that at the entrance plane through the FRFT: $\Phi^{(p)}(\vec{r}_2,z) = \hat{F_\alpha}\{\Phi^{(p)}(\vec{r}_1,0)\}\exp(-i\alpha)$.

An arbitrary square-integrable input field can be expressed as a linear superposition of an arbitrary choice of one of the three families of eigensoliton solutions: $\Phi(\vec{r}_1,0) = \Sigma_{p=0}^{\infty} c_p\Phi^{(p)}(\vec{r}_1,0)$. According to the linearity of Eq. (1) and the FRFT, the propagation in SNN media is presented as a FRFT on the input field,

$$\Phi(\vec{r}_2,z) = \hat{F}_\alpha\{\Phi(\vec{r}_1,0)\}\exp(-i\alpha). \tag{6}$$

In the special case $\alpha=\pi/2$, the propagated field at z is deduced as the well-known FT of the input field and reads

$$\Phi(\vec{r}_2,z) = \frac{-i}{2\pi w_c^2}\int\Phi(\vec{r}_1,0)\exp\left(-\frac{i\vec{r}_1\cdot\vec{r}_2}{w_c^2}\right)d^2\vec{r}_1. \tag{7}$$

Equations (5)–(7) indicate that the SNN medium naturally performs a FRFT and FT on the input field. The physical origination of this effect is as follows. When a beam is input into a SNN medium, it induces a quadratic GRIN channel in the medium through nonlocality. The propagation in the channel then performs the FRFT and FT, just as in the traditional quadratic GRIN media [3]. Because the grads of the refractive index distribution can be steered with the power, the order of the self-induced FRFT in the SNN medium can be steered with the input power in addition to the propagation distance z, quite unlike the traditional linear FRFT devices.

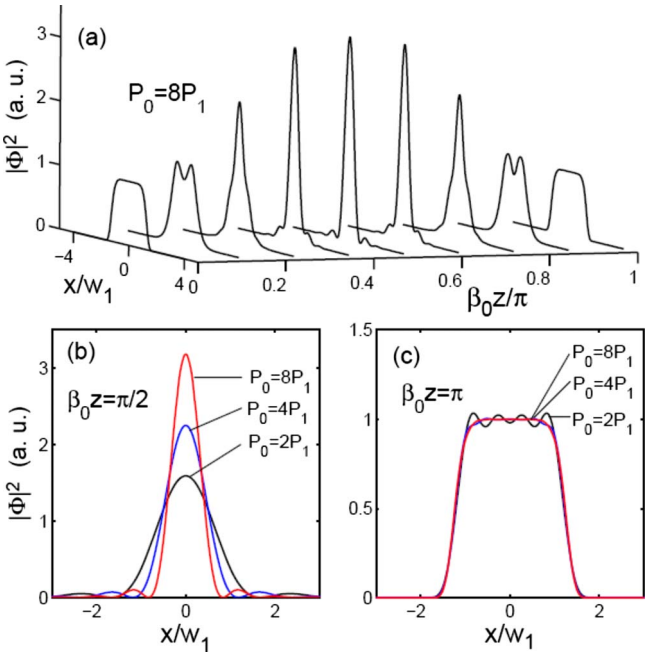

FIG. 1. (Color online) Propagation dynamics of the super-Gaussian field $\exp[-(x/\sqrt{2}w_1)^8]$ in a SNN medium with Gaussian response function $R(r)=1/(2\pi w_R^2)\exp[-r^2/(2w_R^2)]$ [24–26], based on numerical simulation of the NNLSE. (a) Evolution of the profile in propagation. (b), (c) Intensity distributions at $\beta_0 z=\pi/2$ and π, respectively. The nonlocality degree $\Gamma=w_B/w_R=1/10$, w_B is the second-order moment width of the beam at the entrance plane, and P_1 is the critical power for the eigensoliton with generalized width w_1.

The simulation based on the NNLSE shows that the self-induced FRFT becomes more and more distinct with increase of the nonlocality or the input power [Fig. 1(c)]. In fact, the increase of the power is tantamount to the increase of the nonlocality, in that it decreases w_c and the average beamwidth in propagation. On the other hand, the smoother the shape of the input field, the less nonlocality is required to support the FRFT, because it contains fewer higher-order eigensoliton solutions in the superposition. Generally, the profile of the eigensoliton holds when $\Gamma<1/10$. When the order of a constituent eigensoliton in the superposition is high enough so that $\Gamma>1/10$, the profile will be distorted in propagation. Therefore SNN media act as low-pass spatial frequency filters.

Based on the self-induced FRFT, it is convenient to investigate the propagation in SNN media from the viewpoint of Fourier optics. We can predict that the field would present a periodic evolution with the period $\Delta z=2\pi/\sqrt{P_0\gamma}$ (corresponding to $\Delta\alpha=2\pi$) (Figs. 1 and 2). As a result of the cascade of FTs, the pattern evolves to the inversion of the input pattern at $z=(2n+1)\pi/\sqrt{P_0\gamma}$ and revives to the input pattern at $z=2n\pi/\sqrt{P_0\gamma}$ (Fig. 2) (we call those cross sections the revived planes or imaging planes). At

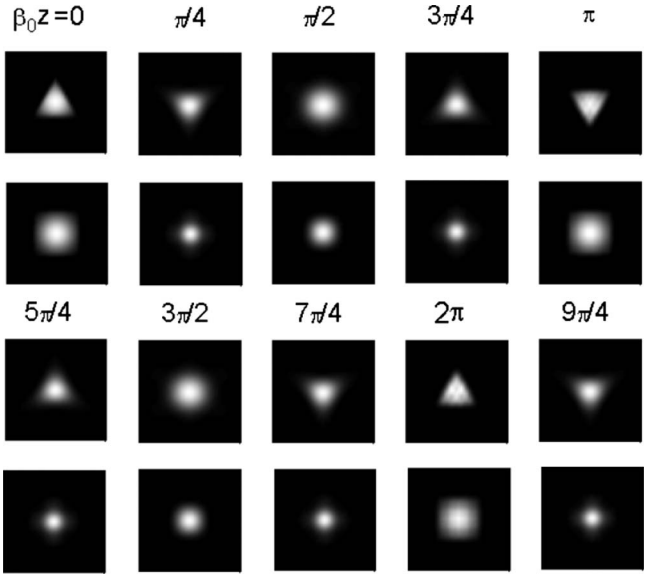

FIG. 2. Propagation dynamics of Gaussian beams $\{\exp[-(x/\sqrt{2}w_1)^2]\}$ truncated by triangular (rows 1 and 3) and square (rows 2 and 4) super-Gaussian diaphragms in SNN media with Gaussian response functions based on numerical simulation of the NNLSE. $P_0=4P_1$. $\Gamma=1/20$.

$z=(n+1/2)\pi/\sqrt{P_0}\gamma$ (we call these cross sections the Fourier planes), the patterns are the FT spectra of the input field or the inversion. From Eq. (7) the spatial frequency $\vec{k}_r=\vec{r}_2/w_c^2$; thus at the Fourier planes the beamwidth $w(z)\propto 1/\sqrt{P_0}$, which obeys the scaling rule of FTs [Fig. 1(b)]. Because of the periodic revivable evolution, which is similar to higher-order temporal solitons in fibers, we call this type of propagation the RHOSS (the RHOSS should be distinguished from the traditionally mentioned "higher-order spatial soliton" which refers to a stationarily propagated multipole spatial soliton). There is an interesting difference between the higher-order temporal soliton in fibers and the RHOSS: the existence of the higher-order temporal soliton in fibers requires much more power than that required for the fundamental soliton, whereas to support the RHOSS, the power can be lower than the critical power for the stationarily propagated fundamental soliton.

According to properties of the FRFT, there are three special cases of the RHOSS (Fig. 3).

(1) Building-block-like soliton. As shown in Eq. (4), during propagation, every degenerate eigensoliton with order p has the same propagation-induced phase $\beta^{(p)}z$ [or, in other words, has the same FRFT eigenvalue $\exp(-ip\alpha)$]. Therefore, when (i) the input field is the linear superposition of the eigensoliton solutions with the same order p, beam center, and generalized width w_1, and (ii) the power is the critical power $P_1=1/(k^2w_1^4\gamma^2)$ that supports eigensolitons with generalized width w_1, the field will propagate stationarily, i.e., the soliton occurs (rows 1 and 2 in Fig. 3). Because a field of this type can be freely composed of eigensoliton solutions with the same order, we call it a building-block-like soliton.

(2) Building-block-like breather. When all are the same as the building-block-like soliton except the input power P_0 deviates from the critical power P_1, the FRFT keeps the shape

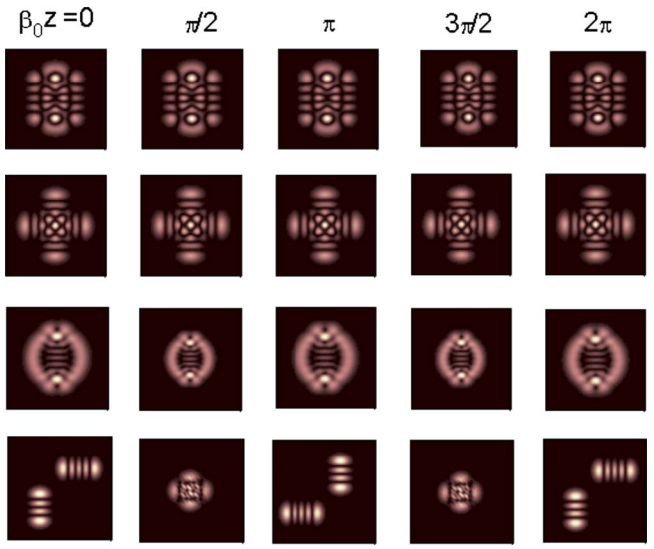

FIG. 3. (Color online) Propagation dynamics of building-block-like soliton (rows 1 and 2), building-block-like breather (row 3), and multisoliton interaction (row 4) in SNN media with Gaussian response function based on numerical simulation of the NNLSE. $\Gamma=1/10$, $P_0=2P_1$ for row 3, and $P_0=P_1$ for the others. The input fields are respectively $(\mathcal{H}_{4,4}^{(8)}-\mathcal{H}_{0,8}^{(8)}/10)$ (row 1), $(\mathcal{H}_{0,8}^{(8)}+\mathcal{H}_{8,0}^{(8)})$ (row 2), $(\mathcal{L}_{8,0}^{(c,8)}+i\mathcal{L}_{8,0}^{(s,8)}-\mathcal{H}_{0,8}^{(8)}/125)$ (row 3), and $[\mathcal{H}_{0,3}^{(3)}(x+3w_1,y+3w_1)+\mathcal{H}_{4,0}^{(4)}(x-3w_1,y-3w_1)]$ (row 4). The generalized widths of all constituent beams are w_1 at the entrance plane.

of the input field and periodically varies its width with the period $\Delta\alpha=\pi$. Subsequently the evolution is presented as a breather with the period $\Delta z=\pi/\sqrt{P_0}\gamma$ (row 3 in Fig. 3), and the change of the building-block-like breather's width is the same as the prediction for the Gaussian breather in Ref. [14]. At $z=(n+1/2)\pi/\sqrt{P_0}\gamma$, the FRFT is deduced to be the FT and $w(z)\propto 1/\sqrt{P_0}w_1$.

(3) Multisoliton interaction. In this case, the traditional technique might require much effort in mathematical treatment because the orbits of the interacting solitons are influenced by each other. But by introducing the FRFT the evolution of the orbits is presented simply as a shift in the FRFT reads $\Phi(\vec{r}_2,z)=\hat{F}_\alpha\{\Phi(\vec{r}_1-\vec{r}_0,0)\}\exp(-i\alpha)$, where $\vec{r}_0$ represents the initial deviation of the beam center of the interacting soliton from the mass center. Under the vertical incidence condition (row 4 in Fig. 3), the solitons intersect each other at $z=(n+1/2)\pi/\sqrt{P_0}\gamma$, evolve to the inversion $\Phi_{(\vec{r}_0-\vec{r},0)}$ at $z=(2n+1)\pi/\sqrt{P_0}\gamma$, and recur to the input field $\Phi_{(\vec{r}-\vec{r}_0,0)}$ at $z=2n\pi/\sqrt{P_0}\gamma$.

To verify the prediction about the self-induced FRFT (or in other words, the RHOSS), we carried out an experiment in a columned lead glass. The experimental setup is illustrated in Fig. 4. The beam from a Verdi laser is focused by the collimation lens. A diaphragm is placed at the focus and the real image is produced at the entrance plane of the lead glass by the confocal lenses pair. When the input power is adjusted, the intensity distributions at the entrance and exit planes are monitored by imaging the beams onto a charge-coupled device (CCD) camera. The lead glass is 59.8 mm in length and 15.1 mm in diameter. The beam at the entrance of the lead glass is 85×80 μm^2 in size (for the square dia-

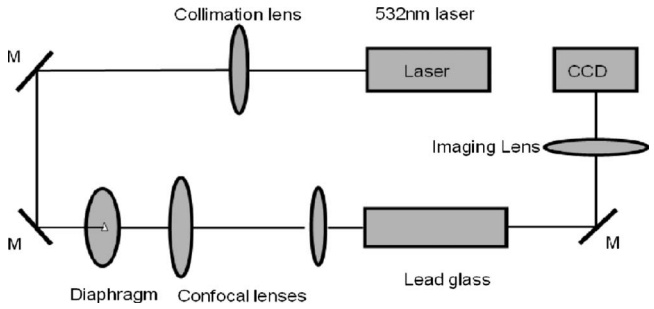

FIG. 4. Sketch of the experiment setup.

phragm) or 106 μm in diameter of the circumcircle (for the triangle diaphragm).

The experimental results are shown in Figs. 5(a)–5(l): by changing the input power, the w_c changes and patterns similar to the FRFT spectra with orders $\alpha=0$, $\pi/4$, $\pi/2$, $3\pi/4$, and π in Fig. 2 are recorded. In the case of the triangle (square) diaphragm, the output pattern reverts to the input pattern when $P_0=551$ mW [Fig. 5(b)] $\{P_0=590$ mW [Fig. 5(h)]$\}$ and evolves to the inversion when $P_0=823$ mW [Fig. 5(f)] $\{P_0=810$ mW [Fig. 5(l)]$\}$. Because the higher frequencies are filtered in propagation, the output patterns are smoother than the input ones. In Fig. 5(z), the variation of the FRFT order α with the square root of the input power, i.e., $\sqrt{P_0}$, is illustrated. The linear fit shows that the FRFT order α is directly proportional to $\sqrt{P_0}$, as predicted in Eq. (5).

In summary, the self-induced FRFT in SNN media causes nonlinear and Fourier optics to intersect with each other. The introduction of the FRFT technique would release one from complicated mathematical calculation in propagation problems such as soliton solutions in SNN media. The RHOSSs,

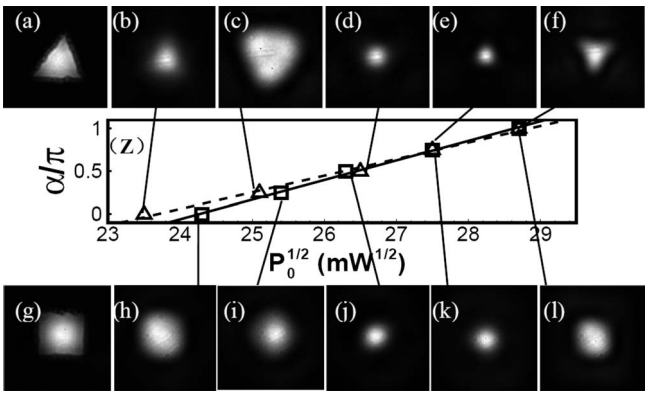

FIG. 5. Experimental results demonstrating self-induced FRFT of Gaussian beams truncated by the triangular (a)–(f) and square (g)–(l) diaphragm at different input powers. (a) and (g) are the input fields, (b)–(f) and (h)–(l) are the output patterns.

including the building-block-like solitons, building-block-like breathers, and their interaction, would greatly enrich the nonlocal soliton family. The fact that the order of the self-induced FRFT in SNN media is related not only to the propagation distance but also to the input power, quite unlike that in traditional linear devices, leads to prospects of new applications of the SNN media such as in developing power-controlled continuously tunable FRFT devices.

This research was supported by the National Natural Science Foundation of China (Grants No. 10674050 and No. 10804033), the Program for Innovative Research Team of Higher Education in Guangdong (Grant No. 06CXTD005), and the Specialized Research Fund for the Doctoral Program of Higher Education (Grant No. 20060574006).

[1] R. N. Bracewell, *The Fourier Transform and Its Applications*, 3rd ed. (McGraw-Hill, New York, 2000).
[2] V. Namias, J. Inst. Math. Appl. **25**, 241 (1980).
[3] D. Mendlovic and H. M. Ozaktas, J. Opt. Soc. Am. A **10**, 1875 (1993).
[4] M. A. Bandres and J. C. Gutiérrez-Vega, Opt. Lett. **30**, 540 (2005).
[5] Y. J. Cai and F. Wang, Opt. Lett. **31**, 2278 (2006).
[6] A. Shahin, H. M. Ozaktas, and D. Mendlovic, Opt. Commun. **120**, 134 (1995).
[7] P. Pellat-Finet, Opt. Lett. **19**, 1388 (1994).
[8] H. M. Ozaktas and D. Mendlovic, J. Opt. Soc. Am. A **12**, 743 (1995).
[9] A. W. Lohmann, J. Opt. Soc. Am. A **10**, 2181 (1993).
[10] L. M. Bernardo and O. D. D. Soares, J. Opt. Soc. Am. A **11**, 2622 (1994).
[11] M. A. Kutay and H. M. Ozaktas, J. Opt. Soc. Am. A **15**, 825 (1998).
[12] J. Hahn, H. Kim, and B. Lee, Opt. Express **14**, 11103 (2006).
[13] P. A. Franken, A. E. Hill, C. W. Peters, and G. Weinreich, Phys. Rev. Lett. **7**, 118 (1961).
[14] A. W. Snyder and D. J. Mitchell, Science **276**, 1538 (1997).
[15] C. Conti, M. Peccianti, and G. Assanto, Phys. Rev. Lett. **92**, 113902 (2004).
[16] C. Rotschild, O. Cohen, O. Manela, M. Segev, and T. Carmon, Phys. Rev. Lett. **95**, 213904 (2005).
[17] A. Dreischuh, D. N. Neshev, D. E. Petersen, O. Bang, and W. Krolikowski, Phys. Rev. Lett. **96**, 043901 (2006).
[18] A. I. Yakimenko, V. M. Lashkin, and O. O. Prikhodko, Phys. Rev. E **73**, 066605 (2006).
[19] C. Rotschild, M. Segev, Z. Y. Xu, Y. V. Kartashov, L. Torner, and O. Cohen, Opt. Lett. **31**, 3312 (2006).
[20] A. V. Mamaev, A. A. Zozulya, V. K. Mezentsev, D. Z. Anderson, and M. Saffman, Phys. Rev. A **56**, R1110 (1997).
[21] N. I. Nikolov, D. Neshev, W. Królikowski, O. Bang, J. J. Rasmussen, and P. L. Christiansen, Opt. Lett. **29**, 286 (2004).
[22] W. Królikowski, M. Saffman, B. Luther-Davies, and C. Denz, Phys. Rev. Lett. **80**, 3240 (1998).
[23] D. M. Deng and Q. Guo, Opt. Lett. **32**, 3206 (2007).
[24] S. Lopez-Aguayo and J. C. Gutiérrez-Vega, Opt. Express **15**, 18326 (2007).
[25] D. Briedis, D. E. Petersen, D. Edmundson, W. Krolikowski, and O. Bang, Opt. Express **13**, 435 (2005).
[26] D. Buccoliero, A. S. Desyatnikov, W. Krolikowski, and Y. S. Kivshar, Phys. Rev. Lett. **98**, 053901 (2007).
[27] M. Peccianti, C. Conti, G. Assanto, A. D. Luca, and C. Umeton, Appl. Phys. Lett. **81**, 3335 (2002).